Talanta 127 (2014) 204–210

Contents lists available at ScienceDirect

Talanta

journal homepage: www.elsevier.com/locate/talanta

Second order multivariate curve resolution of Fourier transform infrared spectroscopic data of the photo-induced crosslinking of thymine functionalized polymers

Santiago A. Bortolato [a], Kristin McDonough [b], Richard W. Gurney [b,*], Débora M. Martino [a,*]

[a] Instituto de Desarrollo Tecnológico para la Industria Química (INTEC) (UNL – CONICET) Güemes 3450, S3000GLN Santa Fe, Argentina
[b] Department of Chemistry and Physics, Simmons College, 300 The Fenway, Boston, MA, 02115, USA

ARTICLE INFO

Article history:
Received 6 March 2014
Received in revised form
4 April 2014
Accepted 7 April 2014
Available online 13 April 2014

Keywords:
Photo-induced curing
FTIR
Multivariate analysis
Biopolymers

ABSTRACT

A meaningful characterization of the photo-induced curing process of materials based on styrene monomers functionalized with thymine and charged ionic groups was accomplished using FT-IR spectroscopy in combination with second-order multivariate calibration algorithms. The polymer composition as well as the irradiation dose effects on the photo-crosslinking of copolymer films was experimentally determined. Each FT-IR absorption spectra was decomposed into the contribution of individual species by means of chemometric algorithms. A second-order strategy involving a three-way array for each sample and analyzing all arrays simultaneously was used. Temperature and solvent frequently have a strong influence on the FT-IR peak producing shifts and trilinearity lost. A new methodology to properly pre-align the spectroscopic matrix data is used based on the decomposition of a three-way array via a suitably initialized and constrained PARAFAC model. The chemical reaction mechanism describing the underlying process in terms of identifiable steps was determined. Associated key parameters and equilibrium rate constants that characterize the interconversion and stability of diverse species were predicted. Additionally, it was possible to quantify all the species even in the presence of a non-calibrated compound.

1. Introduction

In recent years, extensive research has been done to design and construct environmentally benign alternatives for currently used toxic synthetic polymers, such as micro and nanostructures that possess functional external stimuli (pH, temperature, light, etc.). Many chemical and physical structures are complicated, and the relationship between the essential properties of the materials and the available experimental data cannot be described by existing theories. Presently, a great deal of attention is focused on the development of models that can be used to predict the attributes of the final materials based on measured properties of the chemical system such as pressure, temperature, infrared, Raman or NMR spectra. In addition, multivariate statistical data analysis has proven to be a powerful tool for the analysis of large chemistry and biochemistry data sets [1].

One of the biggest problems with commercial polymers is the lack of biodegradability and the need of toxic solvents for their preparation and processing. Water soluble copolymers with pendant thymine groups, such as those including 1-(vinylbenzyl) thymine (VBT), have many demonstrated and as yet realized applications as a greener more benign material [2]. The thymine group imparts the ability to immobilize the oligomer or polymer onto surfaces through a 2+2 photodimerization between neighboring thymine units both intra and intermolecularly, resulting in countless applications of this polymer [3–5]. Furthermore, the polymers can be recycled as the photodimerization process can be reversed photolytically or enzymatically [6]. The preliminary kinetic studies of the gellation point of copolymers of VBT and 1-vinylbenzyl triethylammonium chloride (VBA) of varied monomer ratios were achieved through the measurement of the time dependence of the FT-IR spectrum of thin-films of water-soluble VBT copolymers and analysis by a first-order multivariate curve resolution process [7].

Multivariate calibration techniques such as partial-least squares regression or principal component regression are used to build a mathematical model that relates the multivariate response (spectrum) to the property of interest, which can be used to efficiently and effectively predict the property of interest in new samples. The main advantages of using multivariate calibration techniques are that fast, cheap, and non-destructive analytical measurements (such as optical

* Corresponding authors.
E-mail addresses: richard.gurney@simmons.edu (R.W. Gurney), dmartino@santafe-conicet.gov.ar (D.M. Martino).

http://dx.doi.org/10.1016/j.talanta.2014.04.014
0039-9140/

spectroscopy) can be used to estimate sample properties that otherwise would be time-consuming, expensive and destructive. Multivariate calibration allows for accurate quantitative analysis, even in the presence of heavy interference from other analytes, which is particularly important when monitoring chemical processes producing byproducts as yet unidentified.

It is evident that evolving towards the integration of multiple data sets from previously disparate methods into one coherent computational model offers theoretical and practical advantages from an analytical point of view [8–12]. For example, while the zeroth-order univariate calibration cannot detect sample components producing an interfering signal, the first-order calibration that makes use of a data vector per sample can compensate for potential interferents, provided they are included in the calibration set [13]. Furthermore, second order data lead to three-dimensional structures (three-way arrays), which can be decomposed allowing relative concentrations and profiles of the individual components in the different domains to be directly extracted. In this way, analytes can be quantified even in the presence of unknown interferents not included in the calibration set [14]. Second-order data for a given sample can be produced in different ways, either in a single instrument or by resorting to instrument hyphenation. Numerous second-order calibration and analytical applications have been reported in recent years where the data for a group of samples is recorded and processed using available second-order algorithms [12,15–17].

Recently, the photo-induced curing reaction kinetics of VBT–VBA copolymer was determined combining FT-IR spectroscopy and a multivariate curve resolution assisted by alternate least squares (MCR-ALS) [7]. Following the changes on the carbonyl IR peak associated to the thymine moiety, the photo-dimerization reaction was monitored. Both simulated and experimental systems were analyzed to show the capability of the method in determining the species and kinetic profiles present in the photo-induced crosslinking reaction. However, only qualitative information was obtained and the relative concentrations of the reaction components were not established. The applied first order data processing was likely the limiting factor, because this method detected the presence of an interferent and as a result excluded the possibility of quantification.

A second-order strategy involves generating a three-way array for each sample (in our case, irradiation time, wavenumber and absorbance) and analyzing all arrays simultaneously. However, determining the inner structure of a three-way array is the essential step before choosing a suitable resolution method. Some models such Parallel Factor Analysis (PARAFAC) [18] or Direct Trilinear Decomposition (DTD) [19] require uniform presentation of data, i.e. that each chemical component should present a unique profile in all samples, both in spectral and irradiation time dimensions. Signals obtained by FT-IR or NIR spectroscopy techniques often do not fulfill this requirement since the temperature or the solvent have a strong influence on the peak maximum, producing shifts, and consequentially trilinearity is lost [20]. Conversely, Multivariate Curve Resolution-Alternating Least-Squares (MCR-ALS) [21] or Generalized Rank Annihilation Method (GRAM) [22] are more flexible algorithms, allowing a given component to have different spectral profiles in different samples [23]. However, for systems with large overlap or linear dependence between the components, these algorithms do not solve the problem satisfactorily [24,25]. A potential solution to overcome this drawback is to properly pre-align each matrix data to restore trilinearity in order to apply the above methods [25]. In this work, a new methodology to align the spectroscopic matrix data is used based on the decomposition of a three-way array via a suitably initialized and constrained PARAFAC model. The proposed method is able to properly align the different data matrix, restoring the trilinearity required to process the calibration and test data with second-order multivariate calibration algorithms [25].

In summary, this work presents an experimental study of polymer composition as well as irradiation dose effect on the crosslinking of VBT copolymer films coated on reflective substrates using FT-IR spectroscopy. To this effect, copolymer mixtures of different VBT–VBA compositions were irradiated at 254 nm for different times, and the IR spectra in the region of 400–4000 cm^{-1} was recorded. The total signal of each FT-IR absorption spectra was decomposed into the contribution of individual species via the chemometric algorithm (MCR-ALS). Contrasting with previously published work [7], it was possible to determine the chemical reaction mechanism describing the underlying process in terms of identifiable steps, together with the associated key parameters as well as the rates and/or equilibrium constants that characterize the interconversion and stability of diverse species. Furthermore, it was possible to quantify all the species even in the presence of a non-calibrated compound.

Our method is a competitive alternative to traditional techniques currently used to determine the concentration of the species involved in a curing reaction, with added advantages including reduced analysis time, and the elimination of need for sample pretreatment, sophisticated equipment requirements, and use of toxic solvents, among others [26–29]. In addition, the procedure described herein allows the control of the copolymer composition since the method was found to accurately measure the copolymer ratio in the mixture with a performance comparable to the elemental analysis technique.

2. Experimental section

2.1. Monomers and copolymers synthesis and characterization

All reagents were purchased in the purest available form and were used as received. Sodium hydroxide, isopropanol and hexanes were purchased from Fisher Scientific; 4-vinylbenzyl chloride, hydrochloric acid, azobisisobutyronitrile, acetone, triethylamine, 2,6-di-tert-butyl-4-methylphenol, ethanol and dichloromethane were purchased from Sigma Aldrich; thymine (99%) was purchased from Acros Organics. VBT was synthesized from vinylbenzyl chloride and thymine, while VBA was synthesized from vinylbenzyl chloride and triethylamine as described previously [30]. Based on ^{1}H NMR, IR and TLC analysis, the monomeric products were deemed pure enough for the synthesis of the polymers.

To produce water-soluble polymers, VBT was copolymerized in a free radical process with the cationic monomer, VBA. The ratio of the VBT to VBA monomers influences the behavior of the VBT polymeric system and varies depending on the application. Therefore, typical VBT_n:VBA_m with ratios $n=1$ and $m=$ranging from 0.5 through 4 have been synthesized.

2.1.1. VBT_1:VBA_1 copolymer

To a 150 mL beaker, 40.0 mL degassed 2-propanol and finely ground VBT (2.51 g, 1.0×10^{-2} mol) were combined and hand-stirred with a glass rod for 2 min until a white, opaque liquid of milky consistency was observed. In a separate 150 mL beaker, 35 mL degassed 2-propanol and VBA (2.54 g, 10 mmol) were combined and hand-stirred with a glass rod for 30 s until a colorless, clear liquid was observed. To a 1.5 mL Eppendorf tube, azobisisobutyronitrile (AIBN, 0.0240 g, 1.66×10^{-4} mol) was added and subsequently filled with 2-propanol. The resulting solution was vortexed for 2 min and allowed to sit for 1 h. A 500 mL three-neck, round-bottom flask covered in aluminum foil was purged with N_2 gas, and a Teflon-coated magnetic stir bar was added. The VBT and VBA solutions in 2-propanol were added. The solution

was heated to 85 °C and stirred at 450 RPM under N_2 gas until a clear, colorless liquid was observed (about an hour). The heat was lowered to 65 °C, the system allowed to cool to that temperature and the AIBN solution was then added to the flask. The flask was stoppered, and the reaction was run for 20 h under N_2 gas. The three-neck, round-bottom flask was removed from heat and allowed to cool to room temperature. A clear, colorless liquid with a highly viscous consistency was observed. To a 1000 mL beaker, 600 mL of acetone was added and stirred at 960 RPM such that a vortex was created. To the flask, 3.0 mL 2-propanol was added and stirred until an even consistency was achieved. Using a Pasteur pipet, the compound from the three-neck round-bottom flask was added to the stirring acetone, drop-wise, until no more of the compound could be removed. The flask was then suspended above the stirring acetone and allowed to drip into the beaker for 2 h. The stirring was ceased, and the beaker covered with parafilm and allowed to rest. A white cloud of very fine particles was observed settling to the bottom. After 2 h, a thick, white, gum-like substance formed in the bottom of the flask. Approximately 350 mL acetone was decanted off, and the remaining acetone mixture was vacuum filtered using a Buchner funnel and subsequently triturated with additional acetone. The collected solid was dried overnight in a vacuum oven.

Similarly, VBT_1:VBA_m (m=0.5, 0.75, 1.5, 2 and 4) copolymers were synthesized with identical procedures only varying the corresponding ratios of starting monomers. The copolymerization yields of the obtained samples were: VBT_1:$VBA_{0.5}$ (49%), VBT_1:$VBA_{0.75}$ (52%), VBT_1:VBA_1 (67%), VBT_1:$VBA_{1.5}$ (51%), VBT_1:VBA_2 (66%) and VBT_1:VBA_4 (74%). The absence of unreacted monomers was confirmed by Thin-Layer Chromatography and ^{1}H NMR (90 MHz EFT-NMR, Anasazi Instruments).

The average copolymer compositions were determined by elemental analysis on an Exeter Analytical CE 440 analyzer, with the classical modified Pregl/Dumas technique. The measured mass ratios *C*/*N*/*H* were used to calculate the weight ratios of VBT to VBA in each copolymer.

2.2. Copolymer curing: coating preparation, film irradiation and development

Following green chemistry principles, the main goal was to dissolve the samples in pure water whenever possible while avoiding sonication, which reportedly breaks polystyrene backbones [31]. The VBT–VBA polymers with high ratios of VBT are not soluble in pure water, therefore different water/methanol mixtures were used, minimizing the use of methanol. VBT_1:VBA_m copolymers solutions (m/m) were prepared with concentrations that varied for each sample (all saturated): VBT_1:$VBA_{0.5}$ (3.7%), VBT_1:$VBA_{0.75}$ (5.7%), VBT_1:VBA_1 (5%), VBT_1:$VBA_{1.5}$ (5.7%), VBT_1:VBA_2 (5.9%) and VBT_1:VBA_4 (10%).

The monomer ratios and solvent mixtures used in the experiments are outlined in Table 1. To analyze the solvent effect on the infrared spectra the VBT_1:VBA_1 polymer was also dissolved in pure water and pure DMSO. To create the thin films, a 40 μl aliquot of each VBT–VBA copolymer solution was distributed homogeneously on a gold coated glass slide [(1″ × 3″ × 0.040″) with a 50 Å titanium and 1000 Å gold – Evaporated Metal Films Corporation, Ithaca, NY] using a #3 wire-round milled coating rod (R.D. Specialties Inc., Webster NY). The films were dried at room temperature for 1 h and in a vacuum oven (at 80 °C ~20 Torr) for another hour to give a uniform wet thickness of 6.8 μm according to the coating rod specifications [32]. Films were protected from the light throughout the process.

All polymer coated slides were irradiated at room temperature with a UV hand lamp (Spectroline UL, Model ENF 260c, Spectronics Corporation Westbury, NY) at 254 nm from a distance of 1.27 cm for times ranging from 0 s to 180 min, measuring an IR spectrum every 150 s. This process leads to the immobilization of the polymer in response to the irradiation (photo-resist).

Table 1
Vibrational stretching frequencies of the carbonyl IR absorption band (in cm^{-1}) for different VBT_1:VBA_m copolymer ratios in different solvent mixtures at 20 °C.

	Dielectric constant[a]	$VBA_{0.5}$	$VBA_{0.75}$	VBA_1	$VBA_{1.5}$	VBA_2	VBA_4
DMSO	ε=46.70			1701			
MeOH:H_2O (90:10)	ε=36.80	1707					
MeOH:H_2O (65:35)	ε=48.50		1703				
MeOH:H_2O (60:40)	ε=51.53			1698			
MeOH:H_2O (50:50)	ε=56.53				1697		
H_2O	ε=80.40			1691		1695	1693

[a] From Ref. [41].

Since the photo-immobilized copolymer VBT films are very thin, specular reflectance sampling at high grazing angles in FTIR was used for the measurements due to the enhancement of infrared signal [7,33]. FTIR spectra were collected with a Varian Schimitar FTS-800 Spectrometer outfitted with a Pike 80 Degree Specular Reflectance Accessory (80Spec) purchased from Pike Technologies (Madison, WI). Each spectrum was recorded from 400 cm^{-1} to 4000 cm^{-1} with a resolution of 2 cm^{-1}. Triplicates of copolymer thin films of VBT–VBA were prepared and irradiated every 150 s from 0 s to 180 min (74 time points). The IR chamber was purged with N_2 before sampling to eliminate interference from CO_2 and H_2O. The background signal was taken before every sample.

2.3. Chemometric analysis

The complete spectral region was reduced to the 1647–1900 cm^{-1} region (132 points) for chemometric analysis. The experimental data run in triplicate for each composition (VBT_1:$VBA_{0.5}$, VBT_1:$VBA_{0.75}$, VBT_1:$VBA_{1.5}$, VBT_1:VBA_2 and VBT_1:VBA_4) were arranged in one matrix (namely $\boldsymbol{D_{cal}}$) of size 132 × 370 (74 times × 5 samples). The sample of composition VBT_1:VBA_1 was used as "test sample" and was rearranged with $\boldsymbol{D_{cal}}$ to generate the matrix $\boldsymbol{D}$. The spectra recorded in the FTIR spectrometer were saved in ASCII format, and transferred to a PC microprocessor based on AMD Athlon X2 Dual-Core QL-60 (1.90 GHz) for subsequent manipulation.

All calculations were made using in-house MATLAB 7.0 routines [34], which are available from the authors upon request. The routines used for MCR-ALS were also executed in MATLAB 7.0, and are freely available on the Internet [35]. Chemometric analysis processing took less than 5 min each data matrix.

3. Theory

MCR-ALS model has been discussed in detail elsewhere [12,21,27,36] and therefore only a brief description is presented here. The main and important difference with other published works is that we introduce a pre-process of spectra alignment in order to properly restore trilinearity.

Briefly, the total signal of matrix $\boldsymbol{D}$ obtained from FT-IR spectra is mathematically decomposed into the contribution of individual species, to quantify the content of each component in these three-way arrays [21]. Despite the advantages associated with the multivariate treatment of the spectral data with MCR-ALS, there are some typical problems of the recorded data structure, as it is the case of rank deficiency [21,37]. When the spectroscopic data

derived from chemical systems in evolution it is common to find this rank deficiency, which occurs when the number of sources of variability observed is less than the number of species that absorb in the spectral region analyzed [38,39]. This phenomenon defines how the algorithm should be used, since the first step of its implementation involves the generation of an augmented matrix with the experimental spectra. This augmentation should be done avoiding the rank deficiency. In the studied case, the augmentation was implemented along the irradiation time, where the rank deficiency exists. Thus, the bilinear decomposition for the augmented matrix in the time-augmented mode is performed using the following equation:

$$\boldsymbol{D} = \boldsymbol{G}\boldsymbol{S}^{\mathrm{T}} + \boldsymbol{E} \quad (1)$$

where the columns of $\boldsymbol{D}$ contain the spectra measured for different samples at each irradiation time. The rows of $\boldsymbol{S}$ contain the temporal profiles of the N responsive species involved in all the experiments and the rows of $\boldsymbol{G}$ represent the spectra related to these species. Finally, $\boldsymbol{E}$ is the matrix of the residuals not adjusted by the bilinear decomposition. In the analyzed case, the sizes of these matrices are $\boldsymbol{D}$, J (132 wave numbers) $\times$ K (444=74 irradiation times $\times$ (5 calibration samples+1 test sample)); $\boldsymbol{G}$, $J \times N$; $\boldsymbol{S}$, $K \times N$; $\boldsymbol{E}$, $J \times K$. As can be seen, $\boldsymbol{D}$ contains data for the five calibration samples and for a given test sample.

As discussed above, before processing the matrix $\boldsymbol{D}$, all three-way data were aligned against the VBT_1:VBA_2 sample using the model described in reference [25] to achieve a better resolution via MCR-ALS. Upon completion, the decomposition of $\boldsymbol{D}$ is done through an iterative minimization procedure by alternating least squares of the Frobenius norm of $\boldsymbol{E}$. The minimization is initiated by providing estimated spectra for the different spectral components that are used to estimate $\boldsymbol{G}$ as follows:

$$\hat{\boldsymbol{G}} = \boldsymbol{D}(\boldsymbol{S}^{\mathrm{T}})^{+} \quad (2)$$

where the symbol "^" indicates that it is a matrix estimated from Eq. (1), "T" means the transposed matrix, and the superscript "+" the generalized inverse. From $\hat{\boldsymbol{G}}$, and the original data matrix $\boldsymbol{D}$, the spectral matrix $\boldsymbol{S}$ is recalculated by the least squares:

$$\hat{\boldsymbol{S}} = \boldsymbol{D}^{\mathrm{T}}(\hat{\boldsymbol{G}}^{+})^{\mathrm{T}} \quad (3)$$

$\boldsymbol{E}$ is obtained from Eq. (1) using $\boldsymbol{D}$ and the estimated matrices $\hat{\boldsymbol{G}}$ and $\hat{\boldsymbol{S}}$. These steps are repeated until the convergence is reached. The algorithm is fitted with initial restrictions to achieve greater convergence throughout the process. The system must be non-negative in two dimensions, both in the irradiation time direction and in the wavelength direction.

The MCR-ALS algorithm requires the exact number of factors responsible for the analytical signal, and it is preferable to initialize the system with the profiles of the components as close as possible to the final results. The number of factors is estimated using principal component analysis based on singular value decomposition of the matrix $\boldsymbol{D}$ [12].

Finally, the spectra of the species can be obtained from the analysis of the so-called "pure" spectra, following the method SIMPLe Interactive Self-modeling Mixture Analysis (SIMPLISMA), an algorithm of multivariate resolution that extracts pure spectra from mixtures of variable composition [12,40]. After MCR-ALS decomposition of $\boldsymbol{D}$, concentration information contained in $\boldsymbol{S}$ can be used for quantitative predictions, by first defining the analyte concentration score as the area under the profile for the ith sample:

$$a(i,n) = \sum_{k=1+(i-1)K}^{iK} \boldsymbol{s}(k,n) \quad (4)$$

where $a(i,n)$ is the score for the component $\boldsymbol{n}$ in the sample $\boldsymbol{i}$. The scores represent the normalized contribution of each species in each sample to the absolute signal, and are used to build a pseudo-univariate calibration graph against the analyte concentrations. The graph allows predicting the concentration of a test sample by the interpolation of the obtained test sample score.

4. Results and discussion

The VBT–VBA copolymers were synthesized by varying the feed ratios of both monomers as described in the experimental section. The weight ratios of VBT to VBA in the copolymer were calculated from C/N weight percent ratio determined by elemental analysis (see Table 2).

In a recent work, a deconvolution of the IR spectra (700–1900 cm^{-1}) of VBT–VBA copolymer for different monomer ratios and different irradiation times was carried out using MCR-ALS. The characterization of the crosslinking process of the VBT–VBA copolymer was found to involve four species and the contribution of each species to the total signal at each irradiation time was estimated [7]. However, only qualitative information was obtained and the relative concentrations of the components in the reaction medium were not determined. The method was not sensitive to the existence of species having VBT monomer independent kinetics while being part of the measured signal. The fact that the data processing was performed according to a first order strategy gave rise to the information sparse results. Using a second order strategy, it is possible to determine the chemical reaction mechanism that describes the underlying process in terms of identifiable steps together with the associated key parameters as well as the rates and/or equilibrium constants that define the interconversion and stability of the various species.

The overlaid IR spectra of the carbonyl (C=O) stretching frequency for different VBT–VBA copolymer thin films on a gold coated slide are presented in Fig. 1. The thymine moiety contains two non-equivalent C=O groups, one attached to C_2 and the other attached to C_4; each contributing a unique carbonyl stretching frequency (1684 cm^{-1} and 1700 cm^{-1}) to the spectra. The appearance of only one broad carbonyl peak is explained due to "an average" of all the carbonyl stretching peaks within the copolymer system.

The electronic and vibrational properties of a substance are affected by several microscopic and macroscopic properties of the medium. Consequently, the study of solvent-induced perturbations on characteristic infrared absorption peaks and linear and nonlinear optical properties was of considerable interest. Vibrational frequencies for a molecule depend principally on the dielectric nature of the medium (solvent polarity–dipolarity) when specific local interactions are absent [41]. Specifically, the C=O vibrational stretching frequency in the IR spectra, has been reported to shift toward smaller wavenumbers as the polarity of the solvent increases [42]. The experimental vibrational stretching frequencies of the carbonyl absorption band (in cm^{-1}) for different VBT1:VBA_m copolymers in different solvents and/or solvent

Table 2
Elemental analysis C/H/N weight percent ratio of all VBT–VBA copolymers and calculated VBT_n:VBA_m ratios.

Copolymer	Elemental analysis C/H/N	C/N weight ratio	Calculated VBT_n:VBA_m ratio
VBT_1:$VBA_{0.5}$	60.57/4.23/8.95	6.77	1:0.25
VBT_1:$VBA_{0.75}$	67.84/8.04/8.28	8.19	1:0.95
VBT_1:$VBA_{1.5}$	66.78/8.57/7.56	8.83	1:1.4
VBT_1:VBA_2	61.19/8.77/7.05	8.68	1:1.3
VBT_1:VBA_4	66.87/9.14/6.81	9.82	1:2.5

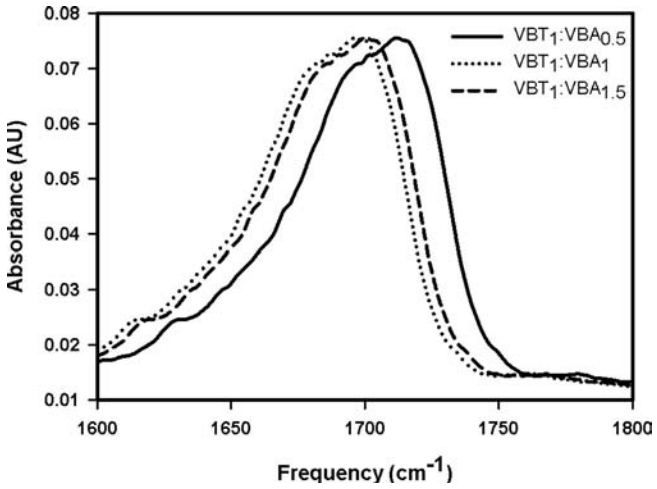

Fig. 1. Grazing angle specular reflectance FT-IR overlaid spectra of the C=O stretching frequency range for unirradiated VBT_1:VBA_m, copolymer thin films on a gold coated slide.

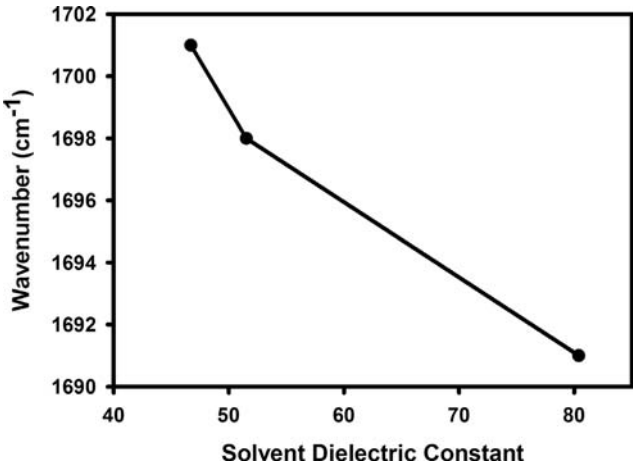

Fig. 2. Solvent effect on the position of the carbonyl vibrational stretching of VBT_1:VBA_1 copolymer in different solvent mixtures.

mixtures at 20 °C are presented in Table 1, together with the dielectric constant of each solvent.

The shift on the C=O vibrational stretching frequency as function of solvent polarity for VBT_1:VBA_1 copolymer (fifth column of Table 1) is clearly visible, Fig. 2. As the solvent dielectric constant increases, the vibrational frequency shifts toward lower wavenumbers. As discussed in the introduction, before carrying out the data analysis using MCR-ALS method the alignment of the data by means of PARAFAC must be completed.

As the UV curing reaction proceeds in the copolymers, the thymine moieties dimerize, resulting in the disappearance of the 5–6 carbon-carbon double bond of the pendant α,β-unsaturated amide of thymine, and the transformation into an α,β-saturated amide. The shift towards higher wavenumbers in the C=O vibrational stretching frequency in the IR spectra, therefore, provides information on the extent of the crosslinking reaction. The predicted MCR-ALS spectra and crosslinking kinetics profiles are shown in Fig. 3 for six different copolymer ratio concentrations. The algorithm was able to suitably resolve the samples, as evidenced by the correct prediction of the number of components present in the mixture and the reasonable determination of the kinetics for each component. The resolved kinetic profiles for all species found by MCR-ALS suggest that the VBT signal decreases as the intermediary is formed, which then disappears to yield the final product, in agreement with previous results [7]. The signal of the species considered as an interferent (VBA) remains constant throughout the crosslinking reaction. As the concentration of the interferent species increases the chemometric resolution worsens, since the relative contribution becomes much more prevalent. However, the results are adequate and the quantitative resolution does not deteriorate (see Fig. 3).

The results obtained with the chemometric algorithm used in this study, not only support the hypotheses concerning the proposed kinetic mechanism in Bortolato et al. [7], but also allow the quantification of the species involved in the reaction even in the presence of an interferent. Additionally, once the decomposition of the total signal in the contribution of individual species is achieved, the time evolution of pure thymine concentration as a function of irradiation time can be used to characterize the kinetics of the curing process.

The predicted MCR-ALS spectra and kinetics profiles for five VBT–VBA copolymer ratios presented in Fig. 3 were used to build the calibration model: VBT_1:$VBA_{0.5}$ (0.66% w/w VBT); VBT_1:$VBA_{0.75}$ (0.56% w/w VBT); VBT_1:$VBA_{1.5}$ (0.39% w/w VBT); VBT_1:VBA_2 (0.32% w/w VBT) and VBT_1:VBA_4, (0.19% w/w VBT). The copolymer ratio VBT_1:VBA_1 of Fig. 3c was used as unknown sample. Results of the calibration model are presented in Fig. 4 for the three meaningful species: VBT, the intermediary species named PHOTO and the final species called PHOTO OX. The concentration of the VBT species in the unknown sample was calculated using the regression curve for VBT in Fig. 4A. In particular, in the test sample VBT_1:VBA_1 the estimated % w/w of VBT was 0.50 ± 0.01

The elemental analysis technique allows the determination of the mass fractions of elements from within the sample: carbon, hydrogen, nitrogen, and heteroatoms (halogens, sulfur). This information is important as it helps determine the structure of an unknown compound, in addition to confirm the purity of a synthesized compound. As shown in Table 2, the elemental analysis results possess some degree of error. The intrinsic experimental error of the elemental analysis technique generally produces atom ratios that are not correct. The accepted deviation of elemental analysis results from calculated values is 0.4%, therefore, in our case an average error of 4% is considered high. An explanation of this observation could be water impurity, given that the VBT–VBA copolymers contain polar groups which can produce strong hydrogen bonding with the solvent of crystallization, being very difficult to remove all the solvent even with the high temperature required by elemental analysis. In addition, the presence of inorganic contaminants or volatile compounds that looses mass after weighing, may explain some of the discrepancies. Even though, the elemental analysis results allow the calculation of the VBT concentration in the test sample VBT_1:VBA_1, obtaining an estimated % w/w of VBT equals to 0.49 ± 0.03 and a showing remarkable agreement with our method.

In a recent work, a characterization of the evolution of the crosslinking process was accomplished using a chemometric algorithm, and a kinetic mechanism was proposed as follows [7]:

$$2\mathrm{VBT} \underset{k2}{\overset{k1}{\longleftrightarrow}} \mathrm{PHOTO} \overset{k3}{\Longrightarrow} \mathrm{PHOTO\ OX};$$

being the reaction speeds:

$$\begin{aligned} dy_{VBT}/dt &= -k_1 y_{VBT}^2 + k_2 y_{PH} \\ dy_{PH}/dt &= k_1 y_{VBT}^2 - k_2 y_{PH} - k_3 y_{PHO} \\ dy_{PHO}/dt &= k_3 y_{PH} \end{aligned} \quad (5)$$

Numerically solving the system of ordinary differential equations [Eq. (5)] using the experimental concentration values and the different rate constants as inputs, the kinetic evolutions were obtained [43]. Those evolutions were compared with the experimental data for all VBT–VBA copolymers, and the rate constants were found to be: $k_1 = 1333\ \mathrm{M^{-1}\,s^{-1}}$, $k_2 = 3\ \mathrm{M^{-1}\,s^{-1}}$ and

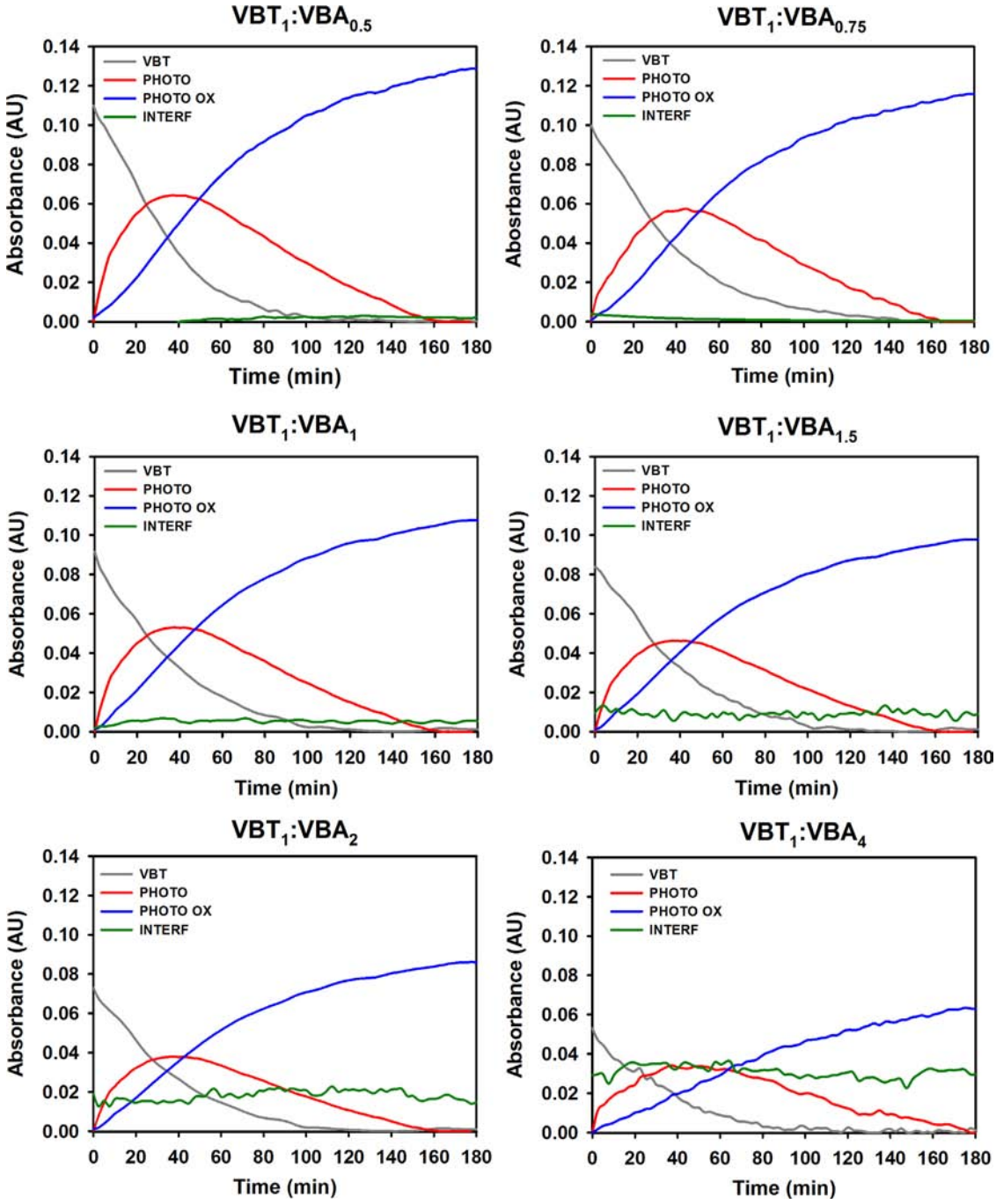

Fig. 3. MCR-ALS spectra and kinetics profiles for six different VBT–VBA copolymer ratios.

$k_3 = 5\ M^{-1}\ s^{-1}$. The small value for k_2 seems reasonable. These results are in remarkable agreement with previously reported kinetic rate values, where a rate of $1030\ M^{-1}\ s^{-1}$ was found using UV–vis as experimental technique [44].

5. Conclusions

A characterization of the evolution of the curing process of VBT–VBA copolymer was studied using FT-IR spectroscopy in combination with second-order chemometric algorithms. The curing process was found to involve three species, which absorb in the spectral region analyzed, and the contribution of each species to the total signal at each irradiation time was estimated. The determination of the number of species involved in the reaction process was relevant to establish the curing conditions necessary to produce a crosslinked polymer.

Our method is a competitive alternative to traditional techniques currently used to determine the concentration of the species involved in a curing reaction, having the added advantages of reduced analysis time, no sample pretreatment, no sophisticated equipment requirement, and no use of toxic solvents, among others. In addition, this procedure gives accurate information on the copolymer composition together with the kinetics of all the species involved. Therefore, it is possible to check if the reaction mixture is contaminated, and even if it is, the reaction mixture can still be quantified. The final goal will be to optimize the synthesis and curing processes to obtain materials with pre-specified properties and quality.

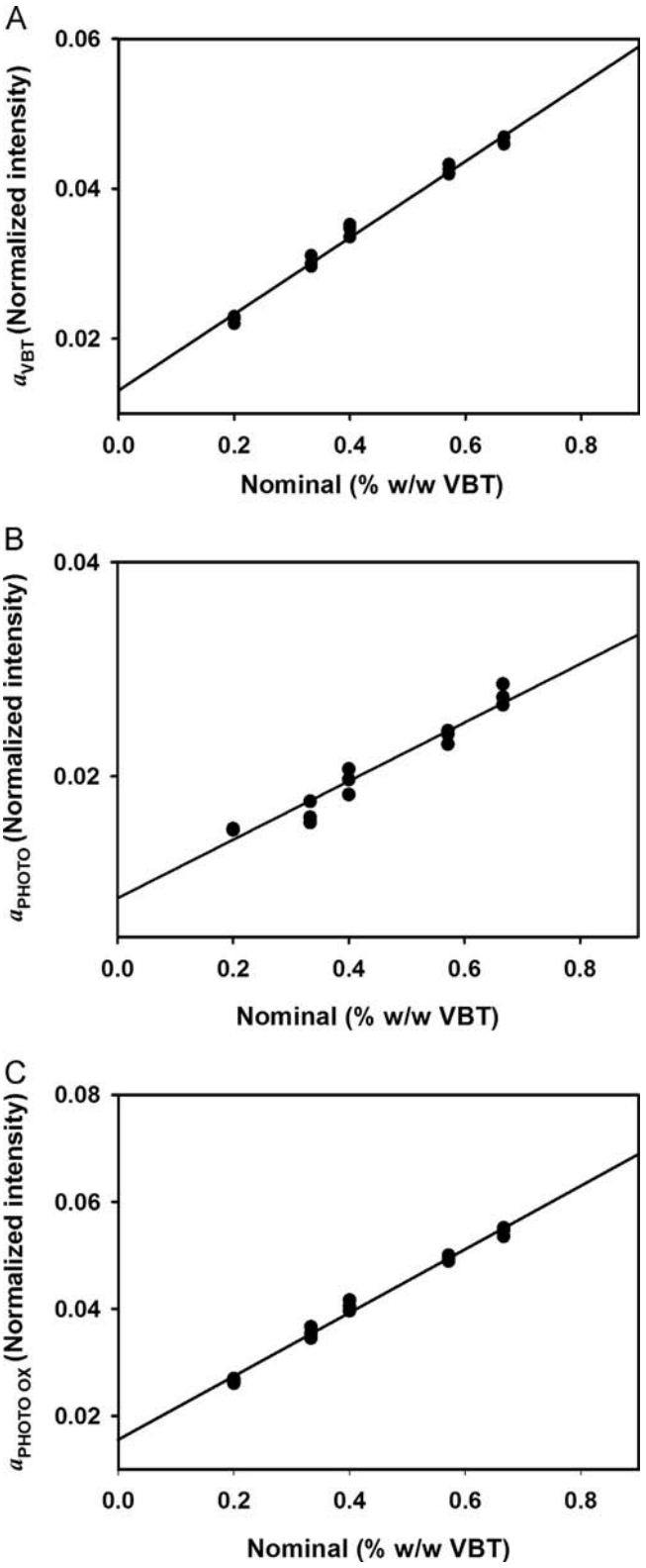

Fig. 4. Calibration curves for the three meaningful species (A) VBT, (B) PHOTO, and (C) PHOTO OX. In all cases, the curves relate the MCR normalized scores (see Eq. (4)) with the nominal concentrations of VBT in the different samples.

Acknowledgments

DMM and SAB are members of the Research Council of CONICET. Authors would like to thank Universidad Nacional del Litoral, Argentina (CAI+D Tipo II PI 11-57), CONICET, Argentina (PIP 112-200801-01079 and D-1280/2011), the NSF OISE USA (#1031394), the Semiconductor Research Corporation USA Educational Alliance-Undergraduate Research Opportunity Program, and the Presidential Fund for Faculty Excellence at Simmons College for the financial support. The Authors further acknowledge the W.M. Keck Foundation for funding the Undergraduate Laboratory Renaissance Program at Simmons College. Special thanks to Joe Genevich for all machining work.

References

[1] A. Smilde, R. Bro, P. Geladi, Multi-way Analysis: Applications in the Chemical Sciences, Wiley, Weinheim, Germany, 2004.
[2] K. Saito, J.C. Warner, Green Chem. Lett. Rev. 2 (2009) 71–76.
[3] V.I. Paz Zanini, F. Tulli, D.M. Martino, B. López de Mishima, C.D. Borsarelli, Sens. Actuators B Chem. 181 (2013) 251–258.
[4] H. Kuang, H. He, J. Hou, Z. Xie, X. Jing, Y. Huang, Macromol. Biosci. 13 (11) (2013) 1593–1600.
[5] G. Kaur, S.L.Y. Chang, T.D.M. Bell, M.T.W. Hearn, K. Saito, J. Polym. Sci. Part A 49 (2011) 4121–4128.
[6] J.C. Warner, A. Morelli, M.C. Ku, Methods of solubilizing and recycling biodegradable polymers containing photoreactive moieties using irradiation, U.S. 3,224,497, 2003, 4 pp.
[7] S.A. Bortolato, K.E. Thomas, K. McDonough, R.W. Gurney, D.M. Martino, Polymer 53 (2012) 5285–5294.
[8] T. Munka, S. Baldursdottira, S. Hietalab, T. Radesa, M. Nuopponenb, K. Kalliomäkib, H. Tenhub, J. Rantanena, C.J. Strachanc, Polymer 13 (2013) 6947–6953.
[9] B.K. Lavine, J. Workman, Chemom. Anal. Chem. 85 (2013) 705–714.
[10] H. Momose, K. Hattoria, T. Hirano, K. Ute, Polymer 50 (2009) 3819–3821.
[11] D.J. Harris, M.K. Alam, Polymer 43 (2002) 5147–5155.
[12] C. Ruckebusch, L. Blanchet, Anal. Chim. Acta 765 (2013) 37–44.
[13] G.M. Escandar, A.C. Olivieri, N.K.M. Faber, H.C. Goicoechea, A. Muñoz de la Peña, R.J. Poppi, Trends Anal. Chem. 26 (2007) 752–765.
[14] K.S. Booksh, B.R. Kowalski, Anal. Chem. 66 (1994) 782–791.
[15] A. de Juan, M. Maeder, M. Martınez, R. Tauler, Chemom. Intell. Lab. Syst. 54 (2000) 123–141.
[16] A.C. Olivieri, G.M. Escandar, A. Muñoz de la Peña, Trends Anal. Chem. 30 (2011) 607–617.
[17] G.M. Escandar, A.C. Olivieri, H.C. Goicoechea, A. Muñoz de la Peña, Anal. Chim. Acta 806 (2014) 8–26.
[18] R. Bro, Chemom. Intell. Lab. Syst. 38 (1997) 149–171.
[19] E. Sánchez, B.R. Kowalski, J. Chemom. 4 (1990) 29–45.
[20] V. Pravdova, B. Walczak, D.L. Massart, Anal. Chim. Acta 456 (2002) 77–92.
[21] R. Tauler, Chemom. Intell. Lab. Syst. 30 (1995) 133–146.
[22] E. Sánchez, B.R. Kowalski, Anal. Chem. 58 (1986) 496–499.
[23] A. de Juan, R. Tauler, J. Chemom. 15 (2001) 749–772.
[24] S.A. Bortolato, J.A. Arancibia, G.M. Escandar, Anal. Chem. 81 (2009) 8074–8084.
[25] S.A. Bortolato, J.A. Arancibia, G.M. Escandar, A.C. Olivieri, Chemom. Intell. Lab. Syst. 101 (2010) 30–37.
[26] M. Garrido, M.S. Larrechi, F.X. Rius, Anal. Chim. Acta 585 (2007) 277–285.
[27] N. Spegazzini, I. Ruisánchez, M.S. Larrechi, Anal. Chim. Acta 642 (2009) 155–162.
[28] M. De Luca, S. Mas, G. Ioele, F. Oliverio, G. Ragno, R. Tauler, Int. J. Pharm. 386 (2010) 99–107.
[29] P.H. Março, R.J. Poppi, I.S. Scarminio, R. Tauler, Food Chem. 125 (2011) 1020–1027.
[30] C.M. Cheng, M.I. Egbe, J.M. Grasshoff, D.J. Guarrera, R.P. Pai, L.D. Taylor, J.C. Warner, Phys. Chem. Imaging Syst. 2 (1994) 810.
[31] Characterization and Analysis of Polymers, Arza Seidel, Wiley & Sons INC, New Jersey, 2008. ⟨http://www.wiley.com/WileyCDA/WileyTitle/productCd-0470233001.html⟩ (accessed 25.11.13).
[32] D.M. MacLeod, in: D. Satas (Ed.), Coating Technology Handbook, Marcel Dekker, New York, 1991.
[33] Pike Technologies, Inc. Measurement of Monomolecular Layers using Specialized FTIR Grazing Angle Accessories; Specular Reflectance – Theory and Applications, 2005.
[34] MATLAB 7.0, The Mathworks, Natick, Massachussets, USA, 2007.
[35] ⟨http://www.ub.es/gesq/mcr/mcr.htm⟩.
[36] J. Jaumot, R. Gargallo, A. de Juan, R. Tauler, Chemom. Intell. Lab. Syst. 76 (2005) 101–110.
[37] M. Garrido, I. Lázaro, M.S. Larrechi, F.X. Rius, Anal. Chim. Acta 515 (2004) 65–73.
[38] R. Tauler, R. Gargallo, M. Vives, A. Izquierdo-Ridorsa, Chemom. Intell. Lab. Syst. 46 (1999) 275–295.
[39] A. de Juan, S. Navea, J. Diewok, R. Tauler, Chemom. Intell. Lab. Syst. 70 (2004) 11–21.
[40] W. Windig, J. Guilment, Anal. Chem. 63 (1991) 1425–1432.
[41] G. Akerlof, J. Am. Chem. Soc. 45 (1932) 4125–4139.
[42] Y.J. Alvarado, J.L. Peña-Suárez, N. Cubillán, P.H. Labarca, J.A. Caldera-Luzardo, F. López-Linares, Molecules 10 (2005) 457–474.
[43] MATHEMATICA 7.0, Wolfram Research, Champaign, Illinois, USA, 2009.
[44] S.A. Bortolato, A.L. Barbarini, R.M. Benitez, D.A. Estenoz, D.M. Martino, Lat. Am. Appl. Res 43 (2013) 329–336.